

# The Comparison of Vibration and Power according to Operation Method of 100W IPM Type Motor

Gyeong-Deuk Lee \*, Eul-Gyu Jo \*, and Gyu-Tak Kim \*

**Abstract** – In This paper, the output characteristics and vibrations were compared and analyzed according to operation method in 100W class. The voltage source is applied only two phase in BLDC drive system therefore commutation torque ripple and imbalance of RMF occurred. Due to this efficiency was significantly degraded because mechanical loss is increased, besides the vibration and noise were greatly generated. The vibration and output characteristics were compared and analyzed according to three phase and BLDC drive system.

**Keywords:** IPMSM, Operation method, Vibration, Loss, Efficiency

## 1. Introduction

In case of BLDC operation method, the motor was flowed only two-phase current. Then, the three-phase drive system significantly increases the torque ripple. Further, the occurred RMF between the stator and the rotor core is elliptically generated. The imbalance of RMF was a source of vibration. As a result, very large vibrations were occurred in BLDC operation method rather than a three-phase synchronous operation method [1]-[2]. In this paper, the vibration and efficiency characteristics were compared and examined according to operation method.

## 2. Torque Characteristic

The specification and shape of the basic model were shown in Table 1 and Fig. 1. The cogging torque minimum model was designed by install notch at the basic model. And, the vibration and the output characteristics were compared according to operation method. BLDC drive system and synchronous drive system were used in the operation method.

In general, the cogging torque is the source of speed ripple and vibration were caused by the torque pulsations. This is the factor of motor performance reduction. In particular, the cogging torque is large, when design of permanent magnet motors must be considered because starting characteristics of the motor were affected. As a

reducing method of cogging torque that are several ways on notch, barrier, split magnet and etc

**Table 1.** The specification of basic model

Item	Specification
Rated speed (RPM)	3200
Rated torque (N·m)	0.4
Pole/Slot	4/6
Air-gap length (mm)	1.2
Winding type	Concentrated winding
Br (T)	1.02
Stack length (mm)	41
Stator diameter (mm)	70

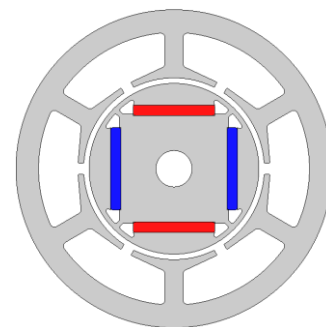


**Fig. 1.** The shape of basic model

In this paper, a notch was formed on the rotor surface. When the cogging torque of minimized, the diameter of the notch was 3.5(mm). The experimental value and calculation value were compared as shown in Fig. 2. As a result, the experimental value is greater than calculation value about 21 (mN·m) based on the peak - peak. This is predicted by the frictional forces of the bearing

\* Corresponding Author: Dept. of Electrical Engineering, Changwon National University, Korea. (gtkim@cwnu.ac.kr)

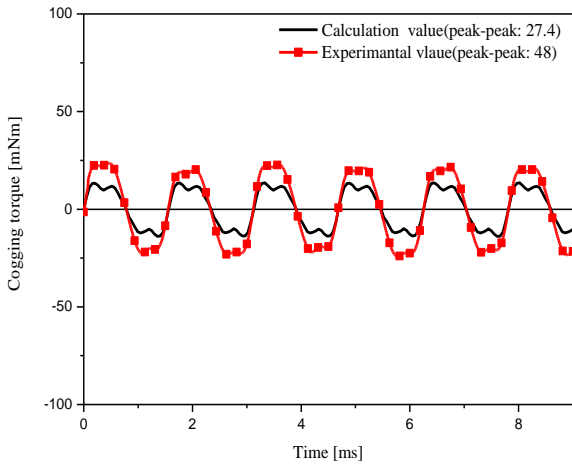
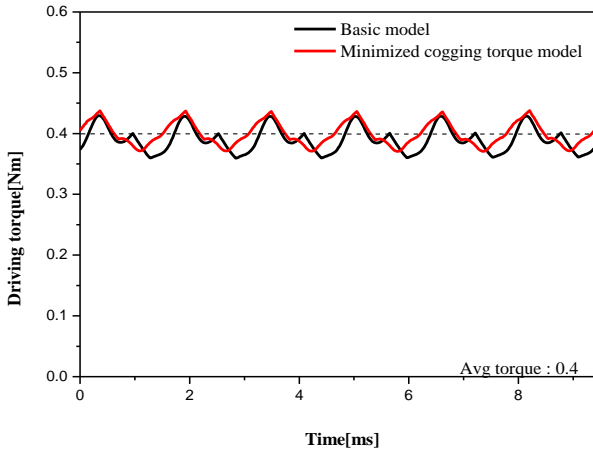
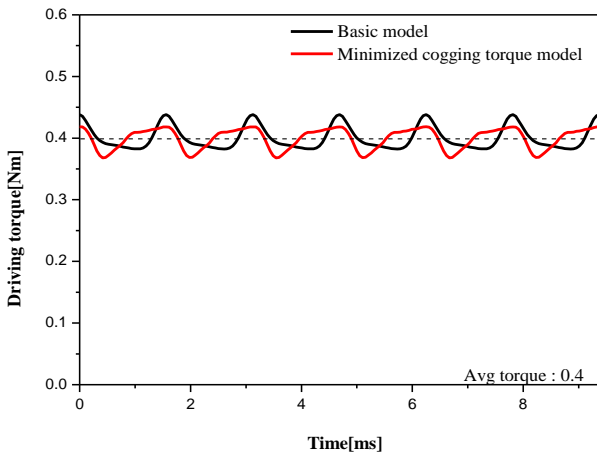


Fig. 2. The cogging torque



(a) BLDC driving mode



(b) Synchronous driving mode

Fig. 3. The operating torque

Torque characteristics according operation method were shown in Fig. 3. As a result of installing notch, the cogging torque has been reduced by 62%. And, when the same torque occurs, the torque ripple was reduced by 0.69% in BLDC operation and 0.93% in synchronous operation.

### 3. Calculation of Iron Loss and Measurement of Mechanical

#### 3.1 Calculation of Iron Loss

(1) responds rapidly to the eddy current loss term, but it does not correspond to hysteresis loss term by the increasing magnetic flux density in the core material and PM. Therefore, the Steinmetz constant is fixed to 2. Because, the magnetic flux density was increased by improvement of the PM and iron core material in electrical machine

$$W_i = W_h + W_e + W_a = k_h f B_m^2 + k_e f^2 B_m^2 + k_a f^{1.5} B_m^{1.5} \quad (1)$$

where,  $f$  is the frequency of the external magnetic field, the  $B_m$  is the maximum value of magnetic flux density,  $k_h$  is the hysteresis loss coefficient,  $k_e$  is the eddy current loss coefficient,  $k_a$  is the abnormal eddy current loss coefficient, and  $n$  is the Steinmetz constants [3].

$$\frac{W_i}{f} = k_e f B_m^2 + k_a \sqrt{f} B_m^{1.5} + k_h B_m^2 \quad (2)$$

Fig. 4 shows Epstein data was divided by frequency such as (2). The iron loss coefficients were estimated for each magnetic flux density. That result was expressed for iron loss coefficients versus magnetic flux density.

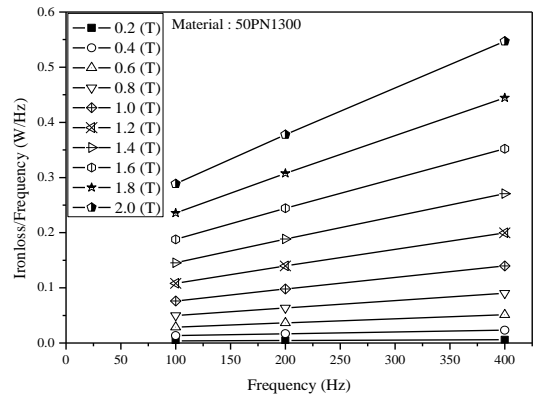


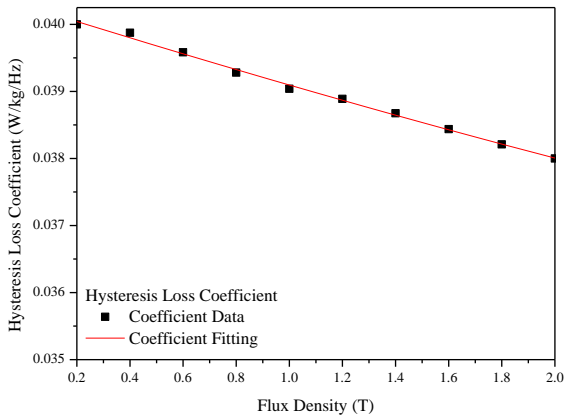
Fig. 4. The iron loss versus frequency according to magnetic flux density

The value of each coefficient is estimated by a cubic function of the magnetic flux density as in (3).

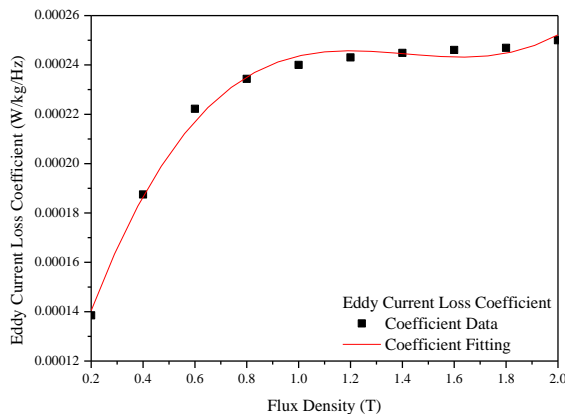
$$k_i = k_{i_0} + k_{i_1} B_m + k_{i_2} B_m^2 + k_{i_3} B_m^3 \quad (i = h, e, a) \quad (3)$$

The value of each coefficient is estimated by a cubic function of the magnetic flux density. Then, the results can

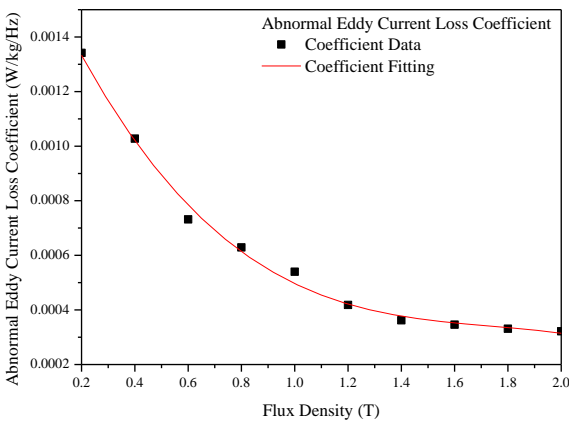
be represented as Fig. 5.



(a) Hysteresis



(b) Eddy current



(c) Abnormal eddy current

**Fig. 5.** Iron loss coefficients calculation according to each flux density

Steinmetz constant was fixed, and the three coefficients were exactly calculated. In other words, Steinmetz constant was fixed by using the provided Epstein data from the manufacturer. As a result, three coefficients were found correctly. And also, the effective air gap was increased

because of the installing notch in cogging torque reduction model. And, total iron loss was reduced because the magnetic flux density was decreased. In operating frequency, hysteresis loss is 20% ~ 30%, eddy current loss is 60% ~ 70%, and abnormal eddy current losses was 10% in the total iron loss [4]-[5]. The iron loss ratios to verify the iron loss coefficient calculation were shown in Table 2.

**Table 2.** Calculated result of the iron loss

Model	Basic model		Cogging torque minimized model	
	(W)	(%)	(W)	(%)
Total iron loss	5.54	100	5.41	100
Hysteresis loss	2.68	48.41	2.58	47.84
Eddy current loss	1.97	35.52	1.93	35.6
Abnormal eddy current loss	0.89	16.07	0.90	16.56

**3.2 Measurement of Mechanical loss**

Fig. 6 shows the mechanical loss Measurement system. The motor was driven by an inverter and Power analyzer to measure the input power was installed at the output section of the inverter. The friction loss between the bearing and the shaft and the windage loss caused by the friction between the rotating rotor and the air are included in the mechanical loss.

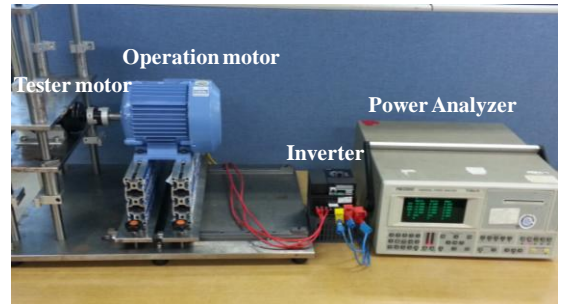


**Fig. 6.** Experiment equipment of the mechanical loss

Mechanical loss must be measured by a motor with the non-magnetized rotor. But taking into account the production period of the permanent magnet Mechanical hand was measured by subtracting the iron loss from the input of the experimental motor.

Iron loss calculated in Table 3 subtracted from the measured input into the operating motor connecting the experimental motor is the mechanical loss.

As a result, the mechanical loss of the basic model is 5.20(W), the mechanical loss of minimized cogging torque model is 4.80(W). Reduced Cogging torque caused the friction loss to decrease. For this reason, mechanical loss

was somewhat reduced.

**Table 3.** Result of the mechanical loss experiment

Model	Input (W)	Mechanical loss (W)
Operating motor	51.98	
Basic model	62.72	5.20
Minimized cogging torque model	62.19	4.80

**3.3 Comparison of Efficiency**

The voltage and current waveforms according to the driving method are shown in Fig. 8. The input power was

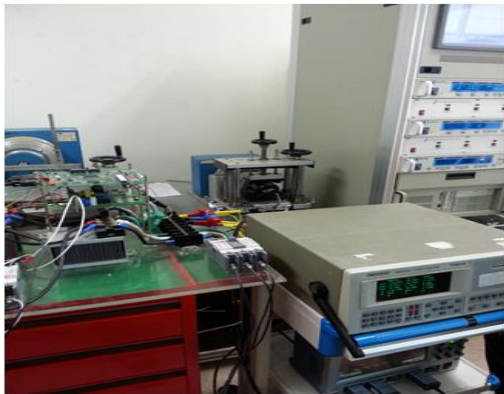
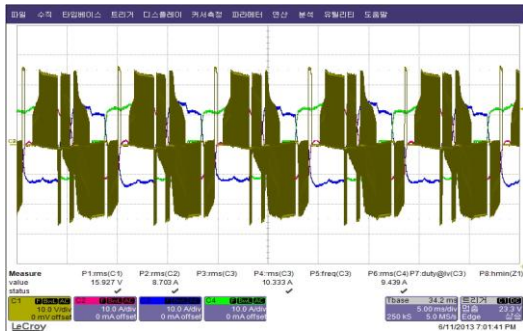
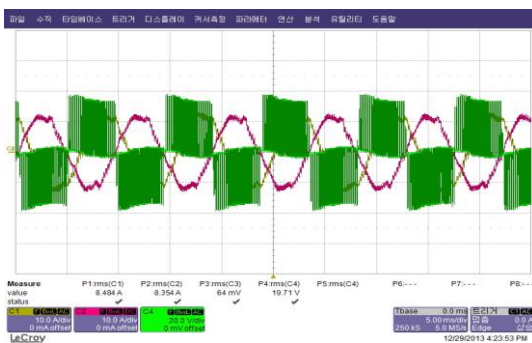


**Fig. 7.** Driving Experiment review



(a) BLDC driving mode



(b) Synchronous driving mode

**Fig. 8.** The experimental waveform

measured by power analyzer (Voltech Co. model PM3300). The maximum efficiency when driving a three-phase was occurred at 4° of the current phase angle and maximum efficiency control was carried out. The BLDC operating characteristics were compared with the 3 phase and the results are shown in Table 4. When driving synchronous mode, the mechanical loss reduction was expected due to the decreased vibration. But it is impossible to measure. So, each loss is separated with the mechanical loss measured by applying No-load regardless of the drive system. Therefore, the stray load losses were significantly reduced when driving synchronous mode.

**Table 4.** The efficiency characteristics according to the driving type

Model	Basic model		Cogging torque minimized model	
	BLDC	Synchr onous	BLDC	Synchr onous
Input (W)	169.2	161.48	171.4	163.04
Torque (N m)	0.4			
Speed (RPM)	3,200			
Output (W)	133			
Copper loss (W)	20.93	16.06	23.2	16.46
Iron loss (W)	5.54	4.67	5.41	4.62
Mechanical loss (W)	5.2		4.8	
Stray load loss (W)	4.53	2.55	5.0	4.16
Efficiency (%)	78.6	83.0	77.6	82.4

**4. Modal Analysis and Vibration Measurements**

**4.1 Modal Analysis**

Mode represents unique dynamic aspects, when stator was vibrated by RMF with any frequency; the behavior of the stator appears through unique mode aspects in frequency band of RMF [6].

Because the natural frequency of stator takes dominant role in vibration and resonance, Modal analysis was performed. Material of the stator is silicon steel (S23-50PN800), it was entered mass density 7850(Kg/m³), mass density 7850(Kg/m³), Poisson ratio 0.24 and Young's modulus 200(Gpa).

Fig. 9 shows the modal analysis results. Compared to other frequency mode it is main mode that generate large vibration and noise therefore should be avoided resonance in elliptical workout mode such as (a) and (b).

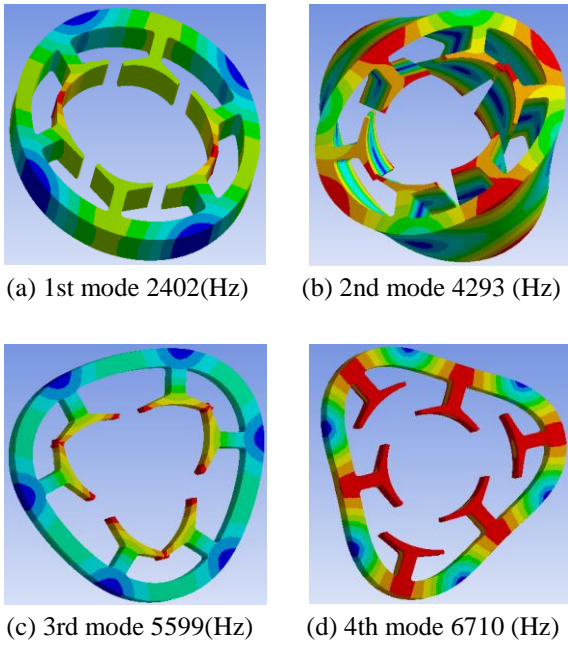


Fig. 9. Mode shape about natural frequency

4.2 The Calculation of the RMF

The source of electromagnetic vibration and noise are generated by radial force density of stator’s surface from air-gap magnetic field in the open-circuit or on-load. The radial force density can be calculated by Maxwell’s stress tensor method as (4)

$$F_{rad}(\theta_s, t) = \frac{1}{2\mu_0} [B_r^2(\theta_s, t) - B_\theta^2(\theta_s, t)] \quad (4)$$

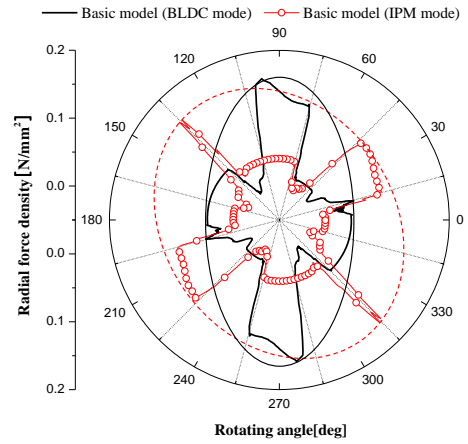
Here,  $F_{rad}$  is the radial component of force density,  $B_r$  and  $B_\theta$  are radial and tangential components of the air-gap flux density,  $\mu_0$  is permeability of free space,  $\theta_s$  is the angular position and  $t$  is the time [7].

Fig. 10 was result that compare distribution pattern of RMF. The more RMF pattern was similar to the circle, the more was balanced. So, an aspect ratio of major axis and minor axis were calculated. Compared to the BLDC driving method on the basic model, an aspect ratio of major axis of the synchronous driving method was more similar to the circle. To calculate the axial ratio of the minimized cogging torque model, the axial ratio is 0.43 on the BLDC driving; the axial ratio is 0.70 on the synchronous driving. So, the aspect ratio of the minimized cogging torque model on synchronous driving was more similar to the circle.

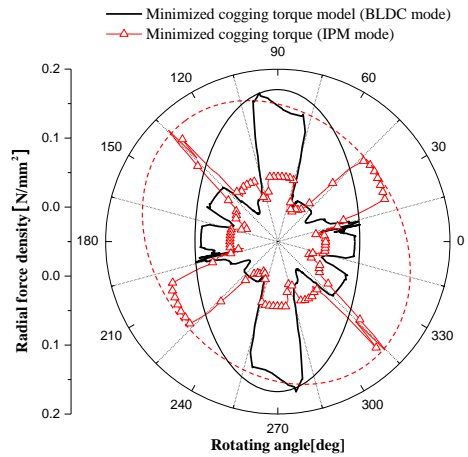
4.3 The Vibration Test

Fig. 11 shows vibration test equipments. The acceleration sensor was used by the PV-97C model. A signal analyzer

was used for SA-01A-4 model. Vibration signal was amplified to use UV-06A amplifier. A vibration signal of shocked by electromagnetic absorbing force was measured in the direction of radiation.



(a) The basic model



(b) The minimized cogging torque model

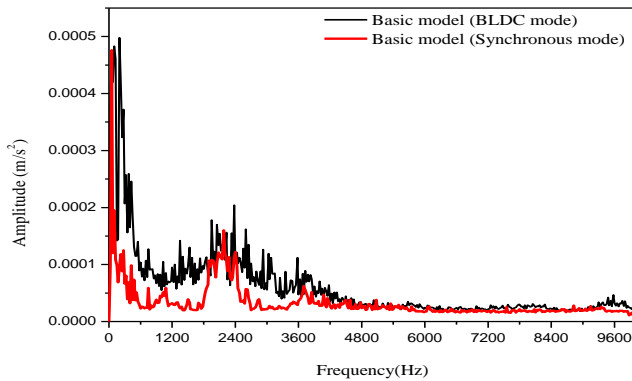
Fig. 10. The distribution of RMF



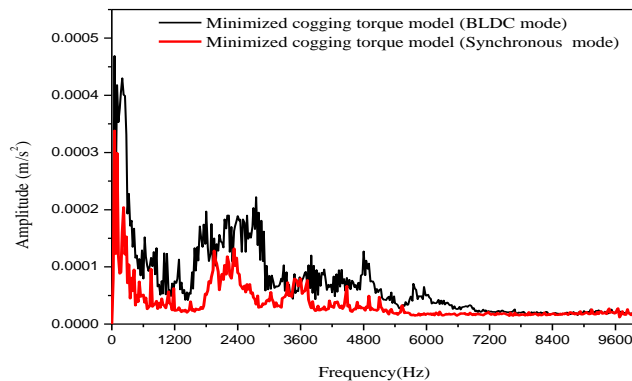
Fig. 11. Experimental measurement and motor

Fig. 12 (a) is the experimental result of the vibration according to the driving method of the basic model and (b) is the experimental result of the vibration according to the driving method of the minimized cogging torque model. When driving BLDC mode, vibration is much bigger than

driving synchronous mode. Unbalanced RMF occurred by BLDC driving causes the vibrations.



(a) The results of the vibration test of the basic model



(b) The results of the vibration test of the minimized cogging torque model

**Fig. 12.** The results of the vibration test

## 5. Conclusion

In this paper, the effect of vibration and the output characteristics related to the unbalanced RMF were analyzed according to the operation method with the 100 (W) class motor. Increase or decrease of the harmonics vibration of the natural frequency mode effects on the vibration amplitude. In order to demonstrate the validity of this study, Vibration experiment was performed. As a result of the experiment, the vibration when driving BLDC mode is largely measured than driving synchronous mode. Unbalanced RMF according to the driving mode affects the vibration. When driving synchronous mode, the efficiency is more than 6% better than driving BLDC mode. A current value for generating the same torque is lower. So the efficiency is higher because of the lower copper loss. In addition, the vibration when driving synchronous mode is smaller. Therefore, the equilibration of the RMF is needed for BLDC driving mode.

## References

- [1] Gyu-Hong Kang, Young-Dae Song, Gyu-Tak Kim and Jin-Hur, "A novel cogging torque reduction method for interior type permanent magnet motor," *IEEE Transaction on. Industry Applications*, vol. 45, no 1, pp 161-167, 2009.
- [2] Tae-Seok Jeong, Gyu-Won Cho, and Gyu-Tak Kim, "The shape design for vibration reduction of IPM type BLDC motor," *19th International Conference on the Computation of Electromagnetic Fields*, PD6-12, 2013.
- [3] Yong-Tae Kim, Bo-Han Kang, Gyu-Won Cho, and Gyu-Tak Kim, "Iron loss coefficient estimation through flux density and iron loss calculation of IPMSM in consideration of core material," *IEEE Conference on Electromagnetic Field Computation*. pp. 233, October, 2012.
- [4] Ping-Kun Lee, Kai-Chen Kuo, Cheng-Ju Wu, Zuo-Tin Wong, and Jia-Yush Yen, "Prediction of iron losses using the modified steinmetz equation under the sinusoidal waveform," *Control Conference (ASCC)*, pp. 579 - 584, 2011.
- [5] Sadowski N, Lajoie-Mazenc M, Bastos J.P.A, Ferreira da Luz M.V, and Kuo-Peng P, "Evaluation and analysis of iron losses in electrical machines using the rain-flow method," *IEEE Transactions on Magnetics*, vol.36, no.4, pp.1923-1926, 2000.
- [6] G. W. Cho, S. H. Woo, S. H. Ji, K. W. Park, K. B. Jang, and G. T. Kim, "The optimization of rotor shape for constant torque improvement and radial magnetic force minimization," *J. Cent. South Univ.Tecnol.*, vol.19, no.2, pp. 357-364, 2012.
- [7] J. F. Gieras, C. Wang, and J. C. Lai, "Noise of polyphase electrical motors", Taylor & Francis Group, 2006.



**Gyeong-Deuk Lee** received B.S degree in electrical engineering from Changwon National University. His research interests are electrical machine and FEM analysis.



**Eul-gyu Jo** received B.S degree in electrical engineering from Changwon National University. His research interests are electrical machine and FEM analysis.



**Gyu-Tak Kim** received B.S, M.S and Ph.D degree in electrical engineering from Hanyang University, Korea. He is presently a Professor of Changwon National University. His research interests are electrical machine and FEM analysis.